Derived band auditory brain-stem response estimates of traveling wave velocity in humans. I: Normal-hearing subjects

Gail S. Donaldson, and Roger A. Ruth

Citation: The Journal of the Acoustical Society of America **93**, 940 (1993); doi: 10.1121/1.405454
View online: https://doi.org/10.1121/1.405454
View Table of Contents: https://asa.scitation.org/toc/jas/93/2
Published by the Acoustical Society of America

Derived band auditory brain-stem response estimates of traveling wave velocity in humans. I: Normal-hearing subjects

Gail S. Donaldson[a] and Roger A. Ruth
Department of Otolaryngology and Communication Disorders Program, Box 430, University of Virginia Health Sciences Center, Charlottesville, Virginia 22908

(Received 9 March 1992; accepted for publication 13 October 1992)

Estimates of cochlear traveling wave velocity (TWV) were computed from derived band auditory brain-stem response (ABR) latencies in 24 normal-hearing subjects. Wave V latencies were determined for each of six derived frequency bands (unmasked–8 kHz, 8–4 kHz, 4–2 kHz, 2–1 kHz, 1 kHz–500 Hz, and 500–250 Hz). Representative frequencies were assigned to the derived bands by estimating their energy midpoints, and cochlear positions corresponding to these frequencies were determined using Greenwood's [J. Acoust. Soc. Am. **33**, 1344–1356 (1961)] place-frequency function for humans. Two procedures were used to estimate TWV. In one procedure, an exponential function of the form $l = A + Be^{Cd}$ was fitted to each subject's latency-by-distance data using a least-squares algorithm, and a TWV function was generated by taking the inverse derivative of the latency function with respect to time. In the second procedure, average TWVs between adjacent derived bands were computed directly from subjects' ipsilateral wave V latencies. Values obtained with the two procedures were similar for middle and apical cochlear loci; however, TWV functions produced lower estimates of TWV at the most basal of five cochlear sites. TWVs based on ipsilateral wave V latencies ranged from 5.6 to 78.0 m/s (geometric mean 11.12 m/s) in the cochlear base (7.53 mm from the stapes) and from 1.2 to 3.4 m/s (geometric mean 1.96 m/s) in the cochlear apex (24.1 mm from the stapes). Intersubject variability was large at the most basal point of TWV estimation but was progressively smaller at more apical sites. Mean TWV estimates were lower than those reported by several previous investigators. The range of values obtained in various studies may stem from differences in the procedures used to estimate TWV.

PACS numbers: 43.64.Ri, 43.64.Kc

INTRODUCTION

Traveling wave velocity (TWV) is the speed with which the amplitude peak of basilar membrane displacement shifts apically in the cochlea during sound stimulation. TWV may be computed from relatively direct measures of cochlear travel time (CTT) in experimental animals. For example, measures of CTT have been obtained by analyzing the latency of cochlear microphonic responses to broadband stimuli at discrete cochlear locations (Tasaki *et al.*, 1952; Teas *et al.*, 1962; Dallos and Cheatham, 1970) and by analyzing the latency of click-evoked auditory nerve fiber responses for fibers of known characteristic frequency (Kiang *et al.*, 1965; Kim and Molnar, 1979). In humans, estimates of TWV must rely on noninvasive and, therefore, indirect measures of traveling wave delay. Such estimates have been obtained using psychoacoustic (Békésy, 1933; Schubert and Elpern, 1959; Zerlin, 1969) and frequency-specific evoked response procedures (Eggermont and Odenthal, 1974; Elberling, 1974; Parker and Thornton, 1978a,b; Hecox and Deegan, 1983; Thornton and Farrell, 1991; Gould and Sobhy, 1992).

Recently, several investigators have used derived band auditory brain-stem response (ABR) latencies to estimate CTT in humans (Parker and Thornton, 1978a,b; Hecox and Deegan, 1983; Thornton and Farrell, 1991; Gould and Sobhy, 1992). In these studies, derived band ABRs are generated using the subtractive high-pass masking procedure of Teas *et al.* (1962): Click-evoked ABRs are masked with a series of high-pass noise maskers having progressively lower cutoff frequencies, and waveform subtraction is performed on adjacent pairs of high-pass masked responses. This yields a set of derived band ABR waveforms, with each waveform presumed to reflect the activity of cochlear elements along a restricted segment of the basilar membrane that is roughly defined by the cutoff frequencies of the corresponding high-pass maskers. Waveform latencies increase with decreasing derived band frequency, reflecting increases in CTT that occur with progressively more apical stimulation. Wave V latencies are typically used to estimate cochlear travel time, because wave I and other earlier waves are often indistinguishable in low-frequency derived band waveforms. It is assumed that factors other than cochlear travel time that contribute to wave V latency, including synaptic delays and central conduction time, are frequency independent. Don and Eggermont (1978) have established the frequency independence of central conduction time in derived band responses of normal-hearing subjects.

Derived band ABRs are readily obtained in human subjects, and response latencies appear to provide dependable

[a] Present address: North Carolina Eye and Ear Hospital, 1110 W. Main St., Durham, NC 27701.

 0001-4966/93/020940-12$06.00

estimates of cochlear travel time. However, a limited number of velocity estimates may be generated across the frequency range of hearing when the derived band procedure is used. Typically, response latencies are obtained for five adjacent frequency bands, and a single velocity estimate is calculated for each pair of adjacent waveforms. This yields TWV estimates corresponding to four cochlear loci. If response latencies cannot be determined for one or more frequency bands, then even fewer velocity estimates may be generated. Because TWV changes rapidly with cochlear distance (especially in the base of the cochlea), it is difficult to characterize velocity-by-distance functions with so few points.

The significance of estimating TWV in human subjects stems from relationships between TWV and cochlear mechanics. In recent years, it has been established that several important aspects of normal auditory function are determined or influenced by the mechanical properties of the cochlea. TWV is similarly determined by mechanical factors in the cochlea, including elasticity, mass, friction, and coupling (Wever, 1962). Thus, TWV estimates provide information about cochlear mechanics that may be useful in assessing human peripheral auditory function. The potential clinical importance of TWV measures, for example in the detection of endolymphatic hydrops, has already been demonstrated (Thornton and Farrell, 1991). However, systematic data relating TWV, cochlear mechanics, and cochlear pathology are lacking.

TWV measures in impaired ears may be accurately interpreted only in the context of adequate normative data. Normative data with respect to TWV in humans are limited: Although several studies have reported mean TWV data for normal-hearing listeners, these studies have generally evaluated small numbers of subjects. Furthermore, existing data with respect to the intersubject variability of TWV estimates in either human or animal subjects are very limited.

The present study was undertaken with two goals in mind. First, we sought to establish a normative database for TWV estimates in human subjects that included quantitative estimates of intersubject variability. Second, we sought to evaluate a curve-fitting procedure for generating TWV estimates from derived band ABR latencies. Such a procedure could provide continuous estimates of TWV over an extended region of the cochlea and circumvent the problem of missing data points mentioned above.

Our curve-fitting procedure used exponential functions of the form $l = A + Be^{Cd}$ to describe wave V latency as a function of cochlear distance. Evidence that latency-distance functions are approximately exponential in form has been provided by auditory nerve data in cats (Kiang *et al.*, 1965; Kim and Molnar, 1979). In humans, it has been shown that narrow-band estimates of TWV decrease exponentially with increasing distance from the stapes (Eggermont, 1976a; 1976b). This implies that human latency-distance functions are also exponential in form.

I. METHODS

A. Subjects

Twenty-four normal-hearing subjects were evaluated. These consisted of 20 females and 4 males who ranged in age from 23 to 51 years. Subjects satisfied the following otologic and audiometric criteria with respect to the test ear: (1) normal otoscopy, (2) pure tone air conduction thresholds $\leqslant$15 dB HL at octave frequencies between 250 and 8000 Hz, (3) speech discrimination scores $\geqslant$90% for digitized NU-6 word lists presented 40 dB above speech reception threshold, (4) normal tympanometry, and (5) contralateral acoustic reflex thresholds$\leqslant$100 dB HL at 0.5, 1, and 2 kHz.

B. Instrumentation

ABR testing utilized a commercially available evoked response system (Nicolet Pathfinder I Mega) for stimulus generation and response acquisition. An analog filter (Krohn–Hite 3343) was used in conjunction with the evoked response system to generate high-pass (HP) noise maskers.

Rarefaction clicks were produced by routing 100-μs electrical pulses through an earphone (300Ω Telephonics TDH-39, mounted in an MX-41/AR rubber cushion). Clicks were presented at 65 dB HL (99 dB peak-equivalent SPL), and at a rate of 27/s, for all conditions of high-pass masking. Continuous high-pass (HP) noise maskers were generated by routing the wideband noise output of the Pathfinder through the analog filter, with the two filter sections cascaded to produce a nominal 96 dB/oct attenuation. Seven maskers were created by high-pass filtering the wideband noise at 8, 4, 2, and 1 kHz, and 500, 250, and 0.01 [wideband masking (WBM)] Hz. A constant spectrum level of 57 dB, equivalent to 95 dB SPL in the wideband condition, was maintained for all maskers. This level was selected on the basis of pilot experiments that indicated that 85–95 dB SPL wide-band noise was required to just mask the click-evoked ABR in several normal-hearing subjects. Clicks and filtered noise were mixed electrically prior to delivery to the earphone.

ABRs were recorded using gold disk electrodes (Grass E5GH) attached to the subject's scalp at the vertex (C_Z), ipsilateral earlobe (A_i), contralateral earlobe (A_c), and forehead (F_z). Typically, individual electrode impedances measured 1–2 kΩ, and the impedance difference between any pair of electrodes was 1 kΩ or less. Potentials detected by the scalp electrodes were amplified (120 000$\times$), filtered between 50 and 3000 Hz (12 dB/oct filter rolloff), and digitized at a sampling rate of 25 kHz for 20.48 ms following stimulus onset. The use of a high-pass filter setting lower than 50 Hz may have permitted us to capture slightly more energy in low-frequency responses; however, the next lowest setting on our amplifier (5 Hz) proved unusable because it allowed too much low-frequency noise to enter the averager. Waveforms were recorded between the vertex and ipsilateral earlobe ($C_z - A_i$, F_z common) (*ipsilateral* recordings) and between the vertex and contralateral earlobe ($C_z - A_c$, F_z common) (*contralateral* recordings) simultaneously, to improve the likelihood of identifying at least one wave V response in each derived frequency band. The Pathfinder's artifact rejection algorithm excluded signals (e.g., due to muscle or high-amplitude EEG activity) with amplitudes exceeding 95% of full scale voltage beyond the first 2.5 ms of

the response window. Waveforms were stored on floppy disk.

C. Procedures

1. Generation of derived waveforms

High-pass (HP) masked ABRs were obtained for each of seven masker conditions in sequential order: Unmasked (UM), 8 kHz HP, 4 kHz HP, 2 kHz HP, 1 kHz HP, 500 Hz HP, 250 Hz HP and 0.01 Hz HP (WBM). Two sets of ipsilateral/contralateral waveform pairs were acquired for each masker condition, with each waveform representing the averaged response to 3000 click presentations. A third set of waveforms was obtained whenever the first two sets of waveforms replicated poorly. Unmasked and HP-masked waveforms were high-pass filtered at 200 Hz after acquisition, using data analysis software provided with the Pathfinder. Specifically, zero-phase filtering was accomplished by taking the Fourier transform of each time-domain waveform, removing spectral components of the response below 200 Hz, and then constructing a new time-domain waveform by reverse Fourier transformation. The principal effect of filtering was to flatten out the HP-masked waveforms. Because the filtering procedure preserved phase relations among spectral components of the ABR, it was expected to have a neglible effect on waveform latencies. A comparison of wave V latencies for several subjects' filtered and unfiltered HP-masked waveforms verified that this was the case.

Waveform subtraction was performed on adjacent pairs of filtered high-pass masked responses to generate derived band responses corresponding to the following seven frequency bands: UM–8 kHz, 8–4 kHz, 4–2 kHz, 2–1 kHz, 1 kHz–500 Hz, 500–250 Hz and 250 Hz–WBM. Ipsilateral and contralateral responses were processed independently, as follows. Four, six, or nine derived waveforms were generated for each frequency band, depending on whether two or three responses had been obtained under each of the corresponding high-pass masker conditions. This was accomplished by performing waveform subtractions on every pairwise combination of the lower-cutoff-frequency and higher-cutoff-frequency HP-masked responses. The derived band waveforms thus obtained were overlaid on the Pathfinder's screen and plotted. An aggregate waveform representing the composite of the 4, 6, or 9 individual derived band responses was also generated and plotted. Wave V identification was based on both the overlaid and composite waveforms; however, a single measure of wave V latency was always taken from the overlaid, individual responses. Wave V responses were readily identifiable in most high-frequency derived band waveforms and, because responses had narrow peaks, wave V latencies could be measured with little ambiguity. In lower-frequency derived band traces, wave V responses were often more ambiguous. In this case, response latencies for higher- and lower-frequency waveforms were used as a guide in wave V identification. Comparisons of ipsilateral and contralateral traces for the frequency band in question were also helpful. However, if identification of wave V remained uncertain, no response was taken. Wave V responses in lower frequency derived bands were typically broad and symmetrical; latencies for these bands were routinely measured at the peak (center) of the response.

2. Assignment of frequency and position values to derived bands

In order to estimate traveling wave velocity from the ABR latency data, it was necessary to assign a single frequency and corresponding cochlear position to each derived frequency band. [However, frequency and position values were not determined for the 250-WBM band, since latency data for this band were excluded from the data analyses (see below).] Frequency assignments were based on the acoustic derived band profiles shown in Fig. 1. Each derived band was defined by the acoustic spectra of two adjacent HP maskers and a constant lower intensity limit, taken to be − 30 dB relative to maximum earphone output. Only stimulus energy in the upper 30 dB of the earphone's acoustic response was considered, because lower-intensity portions of the stimulus likely contribute little to the click-evoked ABR. The basic strategy used in assigning a frequency value to each derived band was to identify the point along the frequency axis that divided the band into two areas of equal acoustic energy. Total energy inside a frequency band was determined by integrating energy in 10-Hz steps between the low- and high-frequency limits of the band. Once total energy had been computed, a second stepwise integration was performed to identify the frequency that bisected the acoustic energy in the band. This frequency was designated as the representative frequency for the derived band in question. Sound pressure levels were converted from logarithmic (decibel) units (as shown in Fig. 1) to units of absolute sound pressure prior to integration. Thus, the frequency assigned to a given derived band was strongly influenced by the shape of the uppermost portion of that band's acoustic profile. This procedure attempts to compensate for irregularities in the earphone's acoustic response which are likely to influence subjects' physiologic responses. The lower intensity limit of

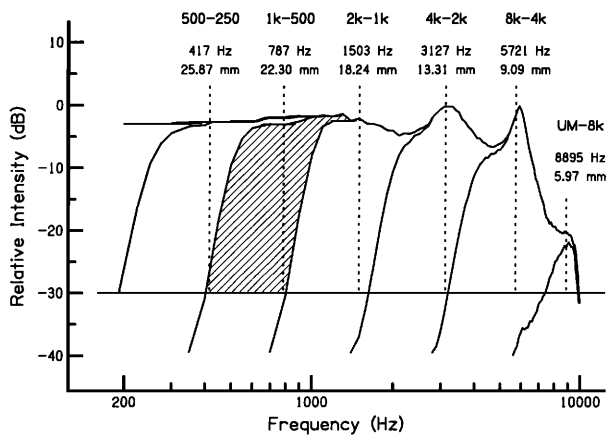

FIG. 1. Acoustic spectra for the six derived frequency bands used in the present study. For illustration purposes, the 1 kHz–500 Hz derived band is shaded. Assigned frequencies and corresponding cochlear positions (mm from the stapes) are indicated for each band.

-30 dB was assigned arbitrarily; however, experimentation with other values (-25 to -45 dB) revealed that frequencies corresponding to the energy midpoints of the six bands changed little ($\pm 2\%$) as the lower limit was varied over a 20-dB range.

Frequencies assigned to each of the six derived bands using the procedure just described are indicated in Fig. 1, together with the corresponding values for cochlear position, specified in mm from the stapes footplate. Cochlear positions were calculated from frequency values using Greenwood's (1961) place map function for humans ($x = 16.7 \log[0.006046f + 1]$, where f is frequency and x is distance from the helicotrema in mm). This function is based on data obtained by Békésy in human cadavers (Békésy, 1960) and not on empirical measurements across the entire frequency range of hearing. However, physiologic data obtained in cats (Liberman, 1982) have shown that Greenwood's (1961) frequency-position function for the cat cochlea is reasonably accurate. By extension, these data support the correctness of the human function used here.

Like Greenwood, we assumed a cochlear length of 35 mm for all subjects. Although histological studies have shown that cochlear length may vary somewhat across individuals within a species (Hardy, 1938; Bredberg, 1968; Bohne and Carr, 1979), we had no means of estimating this value in human subjects. Thus, a constant value for cochlear length was applied in all cases. As explained later, the assumption of constant cochlear length is likely to have reduced intersubject variability for the TWV measures obtained.

3. Latency and TWV functions

Latency-by-distance values corresponding to a maximum of 6 ipsilateral and 6 contralateral wave V latencies per subject were input to a computerized curve-fitting program. The program used a least-squares procedure with equal weighting of data points to fit the latency data with an exponential function of the form $l = A + Be^{Cd}$, where l is latency (ms) and d is distance from the stapes (mm). In this equation, the parameter A governs the asymptotic or shortest latency, B scales the function with respect to cochlear distance, and C controls the rate of growth of the function. Goodness of fit for individual latency functions was assessed with a chi-square (χ^2) statistic.

The cochlear locations actually sampled in acquiring derived band latency data spanned a distance of approximately 20 mm, i.e., 5.97 to 25.87 mm from the stapes footplate (see Fig. 1). However, given the high degree of accuracy provided by the fitted latency functions (see below), it seemed reasonable to extend them slightly beyond this 20 mm range. Accordingly, they were extended 10%, or approximately 2 mm, beyond the most basal and most apical measurement locations. After slight rounding, basal and apical function endpoints were established at cochlear distances 4 and 28 mm, respectively, from the stapes footplate.

A traveling wave velocity (TWV) function was generated from each subject's latency function by taking the inverse of the derivative of the latency function with respect to time. TWV functions are described by the equation $v = 1/(BCe^{Cd})$, where v is traveling wave velocity (m/s), d is distance from the stapes (mm), and B and C are the same constants described earlier.

4. Interband TWV estimates

Estimates of TWV were also generated from subjects' ipsilateral wave V latencies, using a procedure that has become fairly standard in the literature. Interband latencies (differences in wave V latency for responses in adjacent frequency bands) were computed for each pair of adjacent waveforms. This yielded five values per subject when ipsilateral wave V responses were identifiable in all derived bands. Cochlear distances between adjacent bands were determined from the position coordinates specified in Fig. 1, and were the same for all subjects. TWV estimates were then generated by taking the ratio of cochlear distance to interband latency for each pair of derived bands. Each interband TWV estimate represents the average velocity of traveling wave propagation over that segment of the cochlea encompassed by the two derived bands in question. A cochlear position was assigned to each interband TWV estimate by taking the geometric mean of the representative frequencies associated with the adjacent derived bands in question, and then converting the obtained frequency to a position coordinate using Greenwood's (1961) function for humans. For example, representative frequencies corresponding to the 8–4 kHz and 4–2 kHz derived bands are 5721 and 3127 Hz, respectively (see Fig. 1). The geometric mean of 5721 and 3127 is 4229, and the cochlear distance corresponding to 4229 Hz is 11.21 mm. Thus, the velocity estimate computed from the latency shift between the 8–4 kHz and 4–2 kHz bands was assigned to a cochlear position 11.21 mm from the stapes. Following the same procedure, cochlear positions of 7.53, 15.8, 20.3, and 24.1 mm were assigned to the remaining pairs of adjacent derived bands.

II. RESULTS

A. High-pass masked and derived band waveforms

Unmasked and HP-masked responses for a representative subject (DH1) are shown in Fig. 2. Unmasked click-evoked responses were present and highly repeatable for all subjects. Masked responses were typically repeatable for masker cutoff frequencies above 1 kHz, but were less consistent for responses obtained under the 500- and 250-Hz HP conditions. Accordingly, three sets of ipsilateral/contralateral waveform pairs were often acquired under the 500- and 250-Hz HP masked conditions in order to increase the chance of detecting wave V in the 1 kHz–500 Hz and 500–250 Hz derived band ABRs. Wideband masking usually resulted in complete elimination of the click-evoked response; however, a few subjects demonstrated low-amplitude responses under this condition.

Figure 3(a) shows a complete set of derived band responses obtained from the same subject whose HP-masked responses were shown in Fig. 2. For this subject, four responses each were generated for the UM–8 kHz, 8–4 kHz, 4–2 kHz and 2–1 kHz frequency bands, six responses were generated for the 1 kHz–500 Hz band, and nine responses

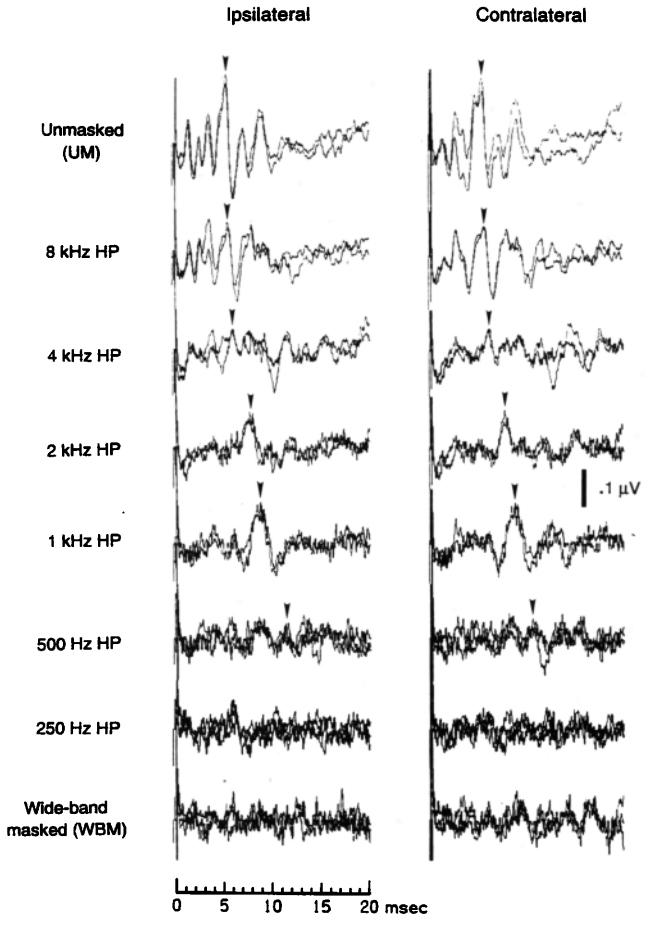

FIG. 2. High-pass masked responses for representative subject DH1. Corresponding ipsilateral and contralateral responses are displayed in the left and right panels, respectively, with masker cutoff frequencies indicated along the left edge of the figure. Responses were digitally high-pass filtered at 200 Hz before plotting. Arrows indicate wave V's.

each were generated for the 500–250 and 250-WBM bands. Composite responses corresponding to the individual, overlaid responses of Fig. 3(a) are shown in Fig. 3(b).

B. Derived band wave V latencies

Wave V latencies increased monotonically with decreasing derived band frequency in all subjects, with the exception that two subjects (MS and AH) exhibited slightly shorter wave V latencies for responses in the 8–4 kHz band than for responses in the UM–8 kHz band. As was the case for the HP masked responses, derived band responses were most robust for frequency bands above 1 kHz (UM–8 kHz, 8–4 kHz, 4–2 kHz and 2–1 kHz). Wave Vs were rarely identifiable for waveforms corresponding to the 250-WBM derived band; therefore, latency measures for this band were excluded from data analyses.

Table I summarizes mean wave V latency data for the 24 subjects tested, as a function of ipsilateral versus contralateral recording condition and derived frequency band. Ipsilateral wave V latencies were slightly but significantly shorter than contralateral wave V latencies in the five highest frequency bands (1-tailed t test, $p<0.05$), however, mean ipsilateral-contralateral differences were nearly constant across frequency (0.05-ms difference for the 4–2 kHz derived band and 0.08–0.09 ms differences for the other four bands). Ipsilateral and contralateral latencies were similar for responses in the 500–250 Hz derived band. Intersubject variability increased with decreasing derived band frequency (as expected due to the increase in overall latency) but was similar for ipsilateral and contralateral responses in a given frequency band.

One subject (HD) yielded unusually short wave V latencies for the 2–1 kHz and 1 kHz–500 Hz derived bands. This subjects' hearing was normal and her ABR data appeared to be valid, however, her TWV function was a clear outlier (see Fig. 6). For this reason, her velocity data were excluded from all group analyses.

Age effects. Correlation coefficients for age versus ipsilateral wave V latency and age versus contralateral wave V latency were computed for each of the six frequency bands included in the analysis. These suggested no systematic correspondence between subject age and derived band wave V latency. Gender effects were not assessed, due to the preponderance of female subjects in our sample.

C. Latency functions

Figure 4 shows the curve-fit latency data for subject DH1. Filled and open triangles represent ipsilateral and contralateral wave V latencies, respectively, plotted at cochlear positions corresponding to the six derived band representative frequencies. There were no missing data points for this subject, since wave Vs were identified in both the ipsilateral and contralateral responses corresponding to each frequency band. The exponential function that provided the best fit to these data was $l = 4.915 + 0.3631\, e^{0.11324d}$. This function is plotted as a solid line in Fig. 4. The latency function closely approximates the measured wave V latencies, and the Chi-square statistic ($\chi^2 = 0.025$, $df = 11$, $p < 0.005$) confirms the excellence of fit. Chi-square values obtained for other subjects' curve-fit data were also extremely small, ranging from 0.005 to 0.155.

Latency functions for the 24 subjects are plotted together in Fig. 5. Function values ranged from 5.36 to 5.94 ms [mean = 5.65 ms, s.d. = 0.19 ms (3.4%)] at their basal end points (4 mm from the stapes footplate) and from 12.10 to 16.02 ms [mean = 13.72 ms, s.d. = 1.06 ms (7.7%)] at their apical end points (28 mm from the stapes footplate). Intersubject variability increased with increasing distance from the stapes footplate.

D. Traveling wave velocity (TWV) data

Individual traveling wave velocity (TWV) functions for all 24 subjects are shown in Fig. 6. Subject HD's function is uppermost in the figure, clearly separated from the other subjects' functions. TWV always decreased with increasing distance from the stapes, as dictated by the exponential function fit to the latency data. TWV function values ranged from 6.89 to 17.25 m/s (geometric mean = 10.9 m/s) in the base of the cochlea (4 mm from the stapes) and from 0.80 to

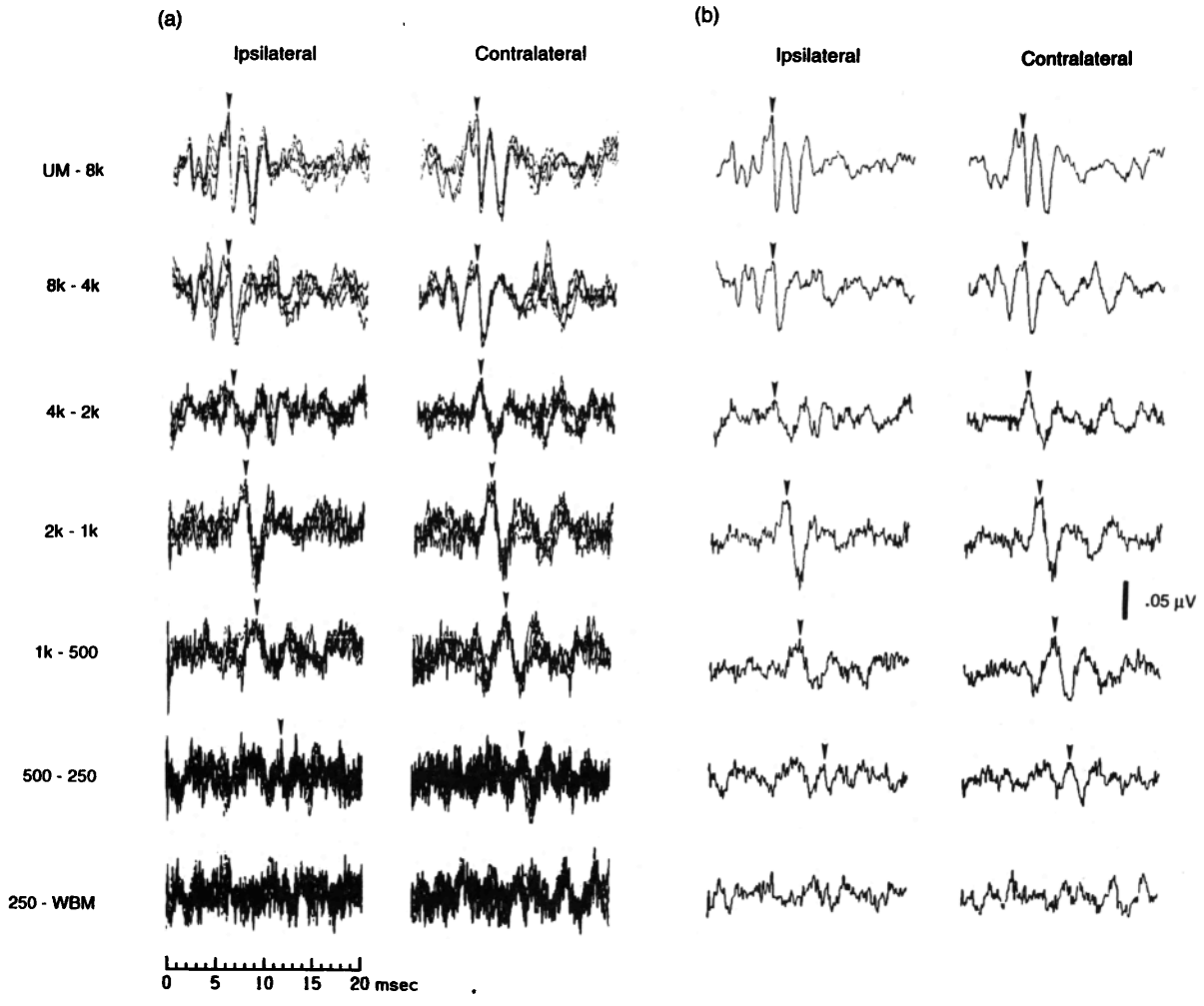

FIG. 3. Derived band responses for subject DH1. (a) individual responses, overlaid. (b) summed responses. In each panel, corresponding ipsilateral and contralateral responses are shown in the left and right columns, respectively, and derived band frequencies are indicated along the left edge of the figure. Arrows indicate wave V's.

1.92 m/s (geometric mean = 1.21 m/s) in the apex (28 mm from the stapes), with subject HD's data excluded.

Figure 7 compares mean TWVs predicted by subjects' TWV functions with mean TWV estimates based on subjects' ipsilateral wave V latencies. Filled triangles represent interband TWV estimates computed directly from subjects' ipsilateral wave V latencies, following the procedure described earlier. Filled circles represent mean values predicted by subjects' TWV functions at the same cochlear positions, i.e., 7.53, 11.21, 15.8, 20.3, and 24.1 mm from the stapes. In each case, error bars represent 95% confidence intervals of the mean. Because both function-based and interband velocity estimates were positively skewed in basal regions of the cochlea, all velocity data were logarithmically transformed prior to statistical analysis.

Table II specifies numeric values for the mean data plotted in Fig. 7 and indicates the number of subjects whose data were included at each cochlear location. As described earlier, subject HD's data were excluded entirely. In addition, data for two subjects (MS and AH, mentioned earlier) were excluded from computations at the most basal (7.53 mm) cochlear location because the ipsilateral wave V latencies

TABLE I. Mean derived band latency data for 24 normal-hearing subjects.

	Ipsilateral wave V latency (ms)						Contralateral wave V latency (ms)					
	UM–8 kHz	8–4 kHz	4–2 kHz	2–1 kHz	1 kHz–500 Hz	500–250 Hz	UM–8 kHz	8–4 kHz	4–2 kHz	2–1 kHz	1 kHz–500 Hz	500–250 Hz
n	24	24	24	23	24	18	24	22	23	22	22	13
mean	5.88	6.17	6.85	8.36	10.02	12.00	5.98	6.26	6.92	8.34	10.10	11.88
s.d.	0.18	0.25	0.35	0.47	0.61	0.66	0.22	0.27	0.333	0.45	0.61	0.74

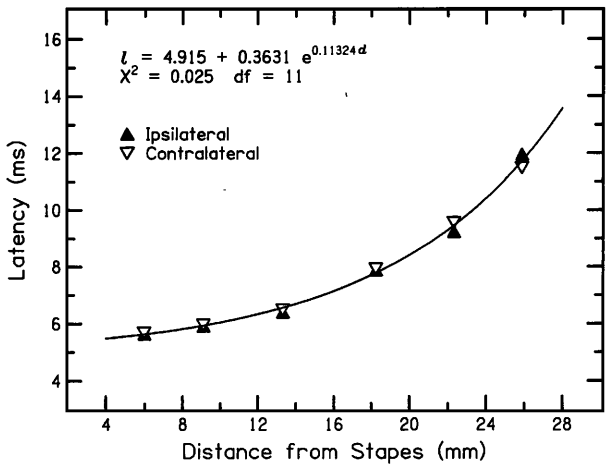

FIG. 4. Curve-fit latency data for representative subject DH1.

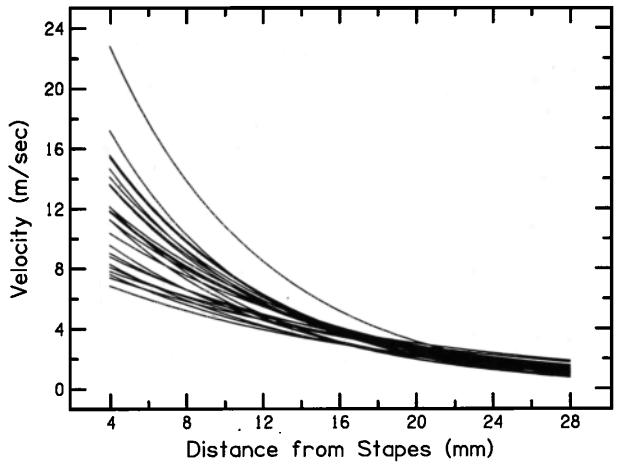

FIG. 6. Individual traveling wave velocity functions for 24 normal-hearing subjects, superimposed.

yielded negative velocity estimates. In addition, interband velocity estimates could not be computed for 1 subject at the 15.8- and 20.3-mm cochlear locations and for 5 subjects at the 24.1-mm cochlear location, due to the absence of ipsilateral wave V responses. In these cases, i.e., where interband velocity estimates were excluded or absent, the corresponding data points for function-based velocity estimates were also excluded. This permitted fair comparisons to be drawn between the two types of TWV estimates.

Several points are evident from Fig. 7. First, TWV functions and ipsilateral wave V latencies produced roughly equivalent mean estimates of TWV; second, the overall variability of interband velocity estimates was much greater than that of TWV functions; and third, the variability of interband velocity estimates was much greater in the base of the cochlea than in the mid-cochlea or apex. Each of these results is considered below.

Statistical analyses of the individual data reflected in

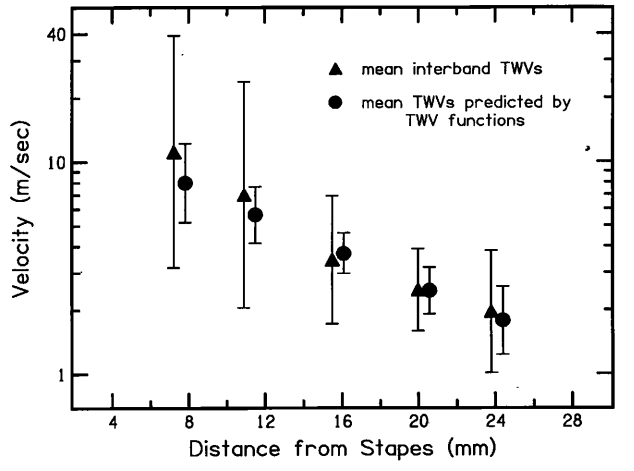

FIG. 7. Group mean data for traveling wave velocity. Filled triangles represent mean TWV estimates computed from subjects' ipsilateral wave V latencies. Filled circles represent mean velocities predicted by the same subjects' TWV functions. Error bars span 95% confidence intervals of the means. Pairs of data points corresponding to a single cochlear position are offset slightly, for purposes of clarity.

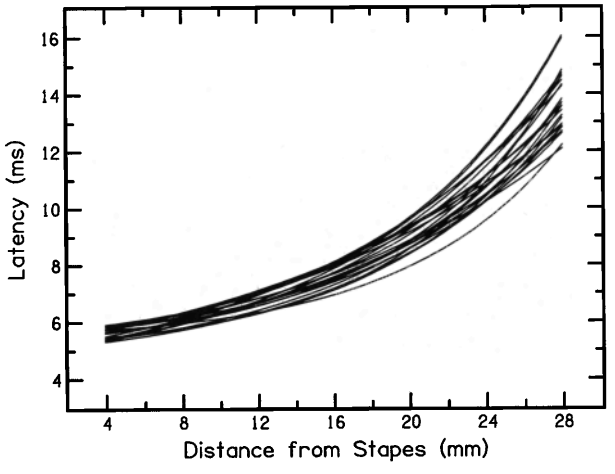

FIG. 5. Individual latency functions for 24 normal-hearing subjects, superimposed.

TABLE II. Mean TWV estimates obtained with two different procedures. Values at the most basal cochlear location (*) are significantly different.

Cochlear position (mm from stapes)	7.53	11.21	15.8	20.3	24.1
mean interband TWV (m/s)	11.14*	6.99	3.45	2.48	1.96
mean TWV predicted by TWV functions (m/s)	7.96*	5.63	3.69	2.46	1.78
n	21	23	22	22	18

Fig. 7 confirmed the first observation above, namely that function-based and interband TWVs were generally equivalent. Specifically, the two procedures produced similar estimates of TWV at four of the five cochlear loci. At the most basal cochlear site (7.53 mm from the stapes) velocity estimates predicted by TWV functions were slightly but significantly lower than those computed from ipsilateral wave V latencies (2-tailed t test, $p < 0.05$). This discrepancy reflects the fact that, for a few subjects, latency functions substantially overestimated the amount of wave V latency shift between the UM–8 kHz and 8–4 kHz derived bands.

Our second observation was that interband velocity estimates demonstrated much greater intersubject variability toward the base of the cochlea than in more apical regions. This pattern of variability can be explained by considering the computational formula for interband velocity, i.e., the ratio of cochlear distance to interband latency for a particular pair of derived bands. Cochlear distances between derived bands were relatively constant across frequency (3.12 to 4.93 mm); however, interband latencies were much smaller in the base of the cochlea (mean = 0.29 ms between the UM–8 kHz and 8–4 kHz bands) than in the apex (mean = 1.88 ms between the 1 kHz–500 Hz and 500–250 Hz bands). Given this, small individual differences in interband latency necessarily resulted in greater changes to velocity estimates in the base of the cochlea than in the apex, accounting for the increased variability observed in the base. A slightly different way to explain this phenomenon is as follows: The margin of error associated with wave V latency measurements in the present study was 0.04–0.08 ms, even when peak responses were unambiguous. A value of 0.08-ms equates to 25% of the 0.32-ms mean interband latency corresponding to the two highest derived frequency bands (UM–8 kHz and 8–4 kHz), but is equivalent to only 4% of the 1.91-ms mean interband latency corresponding to the two lowest frequency bands (1 kHz–500 Hz and 500–250 Hz). This discrepancy is consistent with the observed increase in variability of interband velocity estimates toward the base of the cochlea.

Our final observation with respect to Fig. 7 was that *overall* variability was much smaller for TWV function data than for interband velocity data. This reflects a smoothing of the latency data by the curve-fitting program used to generate TWV functions. This smoothing reduced variability due to factors such as inconsistent response behaviors, ambiguous wave V morphology and measurement error, as illustrated in Fig. 8.

The upper panel of Fig. 8 shows the curve-fit latency data for subject BB1. Wave V morphology was ambiguous for this subject's 4–2 kHz and 2–1 kHz derived band responses, and, as a result, his discrete latency data demonstrated jitter in the mid-frequency region. The latency function preserved the overall pattern of responses but reduced jitter due to measurement ambiguity. Traveling wave velocity data for the same subject are shown in the lower panel of Fig. 8. Interband velocity estimates are shown as filled triangles connected by dashed lines and the TWV function is plotted as a solid line. Small differences in measured wave V latency translate to large shifts in the discrete velocity estimates. However, these aberrations are not present in the TWV function.

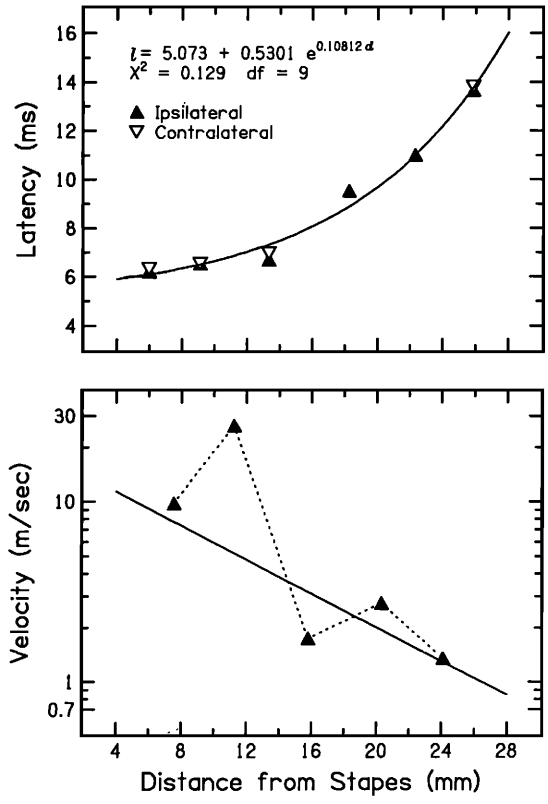

FIG. 8. (a) Curve-fit latency data for a subject (BB1) whose latency function achieved a poorer-than-average fit to the measured wave V latencies. (b) TWV function (solid line) and interband velocity estimates (filled triangles and dashed lines) for the same subject.

The goodness of fit achieved by subject BB1's latency function was the second poorest of any subject studied. Thus, discrepancies between his TWV function and interband velocity data were unusually large. As a point of reference, Fig. 9 shows comparable velocity data for subject DH1. This subject's latency function provided a good fit to

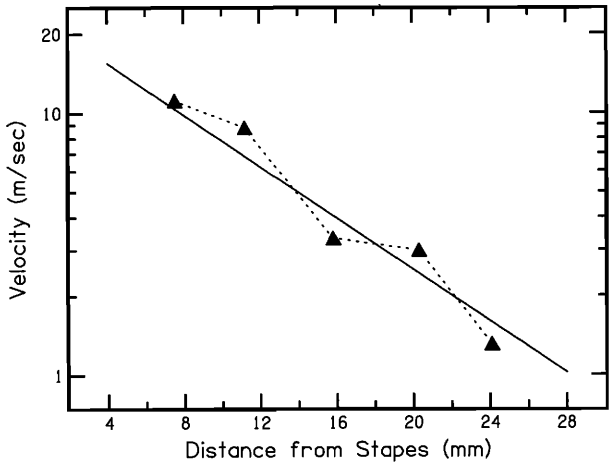

FIG. 9. TWV function (solid line) and interband velocity estimates (filled triangles and dashed lines) for a subject (DH1) whose latency function achieved a better-than-average fit to the measured wave V latencies.

the discrete latency data (see Fig. 4) and, as illustrated in Fig. 9, there was a close correspondence between her TWV function and interband velocity estimates.

III. DISCUSSION

A. Comparisons with earlier data

Mean interband TWVs obtained in the present study and mean velocity data reported by several previous investigators are plotted together in Fig. 10. The present data are shown as filled diamonds. The remaining filled symbols represent mean velocity estimates obtained by other investigators who used derived band ABR techniques (Parker and Thornton, 1978a,b; Hecox and Deegan, 1983; Thornton and Farrell, 1991; Gould and Sobhy, 1992). Unfilled symbols represent mean TWV estimates based on latency data for frequency-specific compound action potentials (Elberling, 1974; Eggermont and Odenthal, 1974), and asterisks represent psychoacoustic velocity estimates (Zerlin, 1969).

TWV estimates obtained in the present study were generally lower than those reported by other investigators. This may be partly attributed to our logarithmic transformation of data, which lowered mean TWV values in the base of the cochlea where data were positively skewed. However, a comparison of geometric (log-transformed) and arithmetic mean values for the present data indicates that differences between the two are small. The largest difference occurs at the most basal (7.53-mm) cochlear site, where geometric and arithmetic mean values for 21 subjects are 11.14 and 14.26 m/s, respectively.

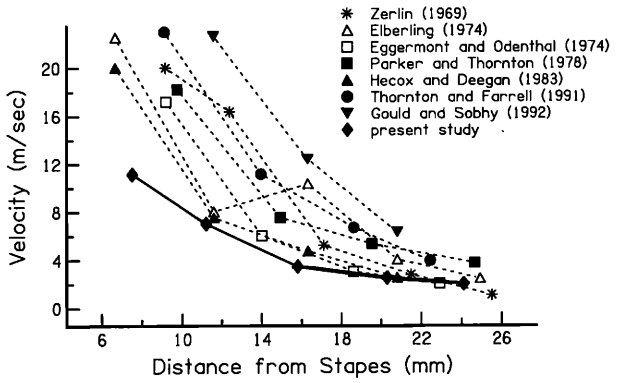

FIG. 10. Group mean estimates for traveling wave velocity (TWV) obtained by several investigators in normal-hearing subjects. Data representing Gould and Sobhy (1992) (downward filled triangles) were computed by the present authors from individual data reported by Gould and Sobhy (1992) for nine subjects who received adequate levels of high-pass masking. Cochlear positions corresponding to mean velocity estimates were determined as follows: For studies which provided a single frequency corresponding to each velocity estimate, frequencies were converted to cochlear distance using Greenwood's (1961) function. When pairs of frequencies were specified (either nominal or actual), unique frequency values corresponding to velocity estimates were generated in one of two ways: (1) If velocity estimates were specified in terms of the adjacent derived bands from which they were generated (e.g., Hecox and Deegan, 1983), the nominal frequency common to the two bands was associated with the velocity estimate. (2) If two discrete-frequency stimuli were specified (e.g., Zerlin, 1969), the geometric mean of those frequencies was computed. Once unique frequencies had been paired with velocity estimates, conversions from frequency to cochlear position were made using Greenwood's (1961) function.

More likely, differences between our mean data and mean values reported by other investigators are due to procedural differences between studies with respect to (1) the assignment of representative frequencies and corresponding cochlear positions to narrow-band stimuli, and (2) the frequency map used in computing cochlear position coordinates and interband cochlear distances. These issues are considered below. In addition, a number of less important procedural issues and subject-related factors (e.g., hearing sensitivity) likely contributed to the differences observed.

In the present study, representative frequencies were assigned to the derived band stimuli using an energy midpoint criterion. (The validity of this procedure is considered below.) Others have used substantially different criteria. Such differences between studies are significant because frequency assignments directly affect cochlear distance computations and, hence, velocity estimates. For example, consider the procedure employed by Parker and Thornton (1978a,b). These investigators defined upper and lower frequency limits for each derived frequency band based on the electrical waveforms of the relevant high-pass maskers and not their acoustic spectra. They took the upper frequency limit to be the half-power frequency of the higher frequency masker, and the lower frequency limit to be the frequency at which the skirt of the lower frequency masker intersected the 0 dB HL point for intensity. For example, upper and lower frequency limits for the 6–3 kHz derived band were taken to be 6000 and 2020 Hz, respectively, given a 60 dB HL stimulus. The geometric mean of the upper and lower limits, in this case 3479 Hz, was taken to be the representative frequency of the derived band.

Parker and Thornton's (1978a) procedure strongly biases frequency assignments in the low-frequency direction, and further assumes that low-frequency, low-energy portions of the derived band are as effective as high-frequency, high-energy portions of the band in eliciting the ABR. Because representative frequencies associated with each band are biased downward, velocity estimates are correspondingly biased toward higher values. We approximated the shapes of masker spectra used in Parker and Thornton's (1978a,b) study, based on their use of a Telephonics TDH-49 earphone, and then recomputed their velocity data using our own frequency assignment procedure. This resulted in a leftward shift of their velocity data along the x axis of Fig. 10 by a distance corresponding to about 2 mm and accounted for nearly half of the overall difference between their data and ours. The source of remaining differences between the two studies is uncertain; however, such differences may stem in part from the fact that Parker and Thornton used ABR waveform components other than wave V to calculate interband latencies.

A second factor that may account for the wide range of mean velocity estimates shown in Fig. 10 is that different studies have employed different cochlear frequency-to-position maps. In estimating TWVs with the derived band technique, cochlear maps are used, first, to determine what coch-

lear distances correspond to particular interband latencies, and, second, to determine what position coordinate should be assigned to each velocity estimate. In Fig. 10, position values associated with particular velocity estimates were consistently determined using Greenwood's (1961) function. However, the actual velocity estimates were based on interband cochlear distances assigned by the respective investigators. Most investigators reported using the human frequency-to-place data of Békésy (1960, 1963) to determine cochlear positions associated with particular frequencies. Greenwood's (1961) function, used in the present study, is also based on Békésy's (1960) data; thus, it would not be expected that discrepancies in velocity estimates would stem from differences in frequency-to-place conversions. However, there are significant differences between Békésy's data as replotted by Zerlin (1969) and that used by Greenwood (1961) to derive his frequency-position function. Comparison of both sets of data to the functions plotted in Békésy's original (1963) paper suggests that Zerlin replotted Békésy's psychophysical data whereas Greenwood modeled Békésy's anatomic (vibration amplitude) data. Gould and Sobhy (1992) estimated interband cochlear distances using the same Békésy map employed by Zerlin (1969) (see below), and a reference in their paper suggests that Parker and Thornton (1978) also used this map. We do not know which data were used by other investigators in making frequency-to-distance conversions. Greenwood's function produces shorter distances between frequency pairs than the psychophysical data of Békésy, especially for frequencies below 3 kHz; thus, it yields relatively lower velocity estimates.

Gould and Sobhy (1992) were unusual among the authors represented in Fig. 10, in that they specified the exact cochlear positions assigned to derived band representative frequencies. To illustrate the extent to which differences in cochlear maps may alter TWV estimates, we compared the interband distances predicted by their position coordinates to interband distances predicted by Greenwood's (1961) function, for the same representative frequencies. This comparison indicated that Greenwood's function would predict TWV estimates 17%, 28%, and 33% lower (from base to apex, respectively) than those computed by Gould and Sobhy (1992) at three cochlear loci (filled downward triangles in Fig. 10). Thus, differences in cochlear frequency-to-position functions account for a significant portion (approximately 20% to 50%, depending on cochlear location) of the difference between their mean data and our own. Even so, these authors reported TWV estimates that were markedly higher than those reported by other investigators. The reasons for this are unclear.

With regard to derived band frequency assignments, it must be emphasized that no one procedure has been proven correct. The energy midpoint criterion used in the present study assumes that, given equal stimulation, the neural elements within a derived band contribute equally to wave V latency. It also implicitly assumes that neural elements are distributed uniformly across each derived band. From a theoretical standpoint, we know of no reason to question the first of these assumptions. However, the second assumption is clearly inaccurate, since innervation densities in the human cochlea are greatest in the 1-kHz region of the cochlea and decline in both higher and lower frequency regions (Spoendlin and Schrott, 1988). Innervation densities predict that derived band wave V latencies would be biased toward the latency of neurons in the 1-kHz region of the cochlea. Thus, latencies for frequency bands above 1 kHz would be prolonged, and latencies for frequency bands below 1 kHz would be reduced, relative to the values expected under conditions of uniform cochlear innervation. However, Burkard (1983) has offered apparent evidence that neural elements toward the high-frequency (basal) limit of any derived band contribute most heavily to response latency. This evidence consists of the following observations: (1) The wave V latency for a given derived band response is usually similar to the wave V latency for a HP-masked click with masker cutoff frequency equal to the upper frequency limit of the derived band. For example, the latency of a 4–2 kHz derived band response is similar to that of a 4-kHz HP masked response. (2) Derived band wave V latencies change little as the lower frequency limit of a derived band is increased or decreased while maintaining a fixed upper frequency limit. Our own mean data support the first of these observations, although the data for several individual subjects deviated from this pattern. Nonetheless, we would hesitate to infer the cochlear place of derived band responses on the basis of HP masked response latencies, since HP responses reflect the combined activity of all stimulated cochlear regions apical to the frequency region of the masker cutoff. Burkard's second observation provides more tenable evidence for a basal weighting of response latencies, although the theoretical basis for this finding is unclear. A possibility is that derived band latencies are weighted toward the 4-kHz region of the cochlea because human hearing is most sensitive in that region.

Procedural issues are especially relevant if TWV data are to be compared across laboratories or if absolute estimates of TWV are at issue. With regard to absolute velocity measures, it should be remembered that derived band estimates of TWV are based on indirect estimates of cochlear travel time and provide, at best, only approximations of *actual* traveling wave velocity. Such estimates may provide useful information with respect to differences between subjects or changes in a given subject over time (i.e., *relative* measures), but are probably not well-suited to absolute velocity determinations.

B. Intersubject variability

An important goal of the present study was to assess the variability of TWV estimates in normal-hearing subjects. In this regard, there were two main findings: First, the variability of TWV estimates was considerably higher in the base of the cochlea than in the apex, for both function-based and interband estimates of TWV. Second, intersubject variability was considerably higher for interband TWV estimates than for function-based estimates of TWV in all regions of the cochlea. Several explanations for these findings were considered earlier.

Some portion of the intersubject variability exhibited by TWV measures in the present study is presumably due to differences in the velocity characteristics of ears studied; however, a number of other factors may also have contributed to this variability. For example, two important assumptions we made as part of our procedure for estimating TWV were that both cochlear length and the cochlear frequency-to-place map were invariant across subjects. Assuming constant cochlear length should have *eliminated* variability in TWV estimates that would have otherwise been introduced by differences in the lengths of subjects' cochleas. On the other hand, individual differences in the cochlear frequency-to-place map would be expected to add to variability. Given that cochlear length is known to vary in humans (Hardy, 1938; Bredberg, 1968), it is indeed likely that there were differences in the cochlear frequency-to-place maps of subjects studied here. Individual differences in subjects' ear canal resonances could also have added to the variability observed for TWV estimates, since our computations of derived band representative frequencies were based on 2-cc coupler measurements of click and high-pass masker spectra and not on real ear measurements in individual subjects.

To our knowledge, only one other study, that of Gould and Sobhy (1992), has explicitly addressed the issue of intersubject variability for TWV. These authors reported TWV estimates for individual subjects, from which measures of variability could be computed. Unfortunately, however, their data are complicated by a secondary issue of undermasking in some subjects, and are difficult to interpret. For the nine subjects whose data were judged by Gould and Sobhy to be valid, intersubject variability was highest in the base of the cochlea and smallest in the apex. This result is consistent with the present findings.

Burkard (personal communication) has suggested that TWV estimates based on derived band evoked response latencies may be contaminated by earphone response characteristics for stimulus frequencies above 4–5 kHz. Since the output of TDH-39 and TDH-49/50 earphones rolls off abruptly at high frequencies, waveform latencies may be prolonged as the result of a reduction in the effective intensity level of the click stimulus. The TDH-39 earphone used here provided fairly constant output for frequencies up to 6 kHz. However, there was nearly 20 dB difference in earphone output between the representative frequencies corresponding to the UM–8 kHz and 8–4 kHz derived bands (see Fig. 1). Don *et al.* (1979) have demonstrated that a 20 dB decrease in click intensity, for example from 70 to 50 dB HL, can significantly increase derived band wave V latencies. Thus, it is possible that our subjects' response latencies for the UM–8 kHz derived band were prolonged relative to those in the 8–4 kHz band due to a reduction in effective click intensity. This would result in artificially shortened latency shifts between the two bands (relative to those expected on the basis of place alone), and elevated velocities. Effective click levels above 6 kHz would also vary according to listeners' high-frequency hearing sensitivity, causing the relative contributions of place and click level to differ between subjects. This factor may well have contributed to the large variability we observed for TWV estimates in the basal cochlea. In theory, it could also account for the fact that two of our subjects demonstrated shorter wave V latencies for the 8–4 kHz derived band than for the higher frequency UM–8 kHz band. Clearly, evoked potential estimates of TWV must be interpreted with caution when earphone output characteristics permit the possibility of click-level effects. With regard to the present data, this caveat is probably relevant for frequencies above 6 kHz.

Intersubject variability was considerably lower for TWV functions than for interband velocity estimates at comparable positions in the cochlea. This presumably resulted from an effective smoothing of individual subjects' latency data by the curve-fitting program. That is, the value of a subjects' latency function at any given cochlear position was influenced by function values at all other positions. It is impossible to know what proportion of the variability exhibited by either TWV functions or interband velocity estimates can be attributed to differences in the mechanical characteristics of subjects' cochleas. However, a review of individual subjects' data suggests that the increased variability of interband velocity estimates relative to TWV function values may be largely attributable to wave V measurement ambiguities. As illustrated earlier (Figs. 8 and 9), subjects whose wave V latencies could be specified with a high degree of certainty yielded interband and function-based TWV values that agreed closely with one another. On the other hand, subjects whose wave V latencies were more equivocal, typically due to ambiguous wave V morphology, yielded interband velocity estimates that fluctuated, sometimes widely, about the TWV function. To the extent that waveform ambiguities affecting wave V latency measurements stem from noncochlear factors, these observations suggest that an important source of noncochlear variability was eliminated by the use of a curve-fitting procedure. If so, then function-based estimates of TWV may permit more effective comparisons of traveling wave velocity between individuals or groups of subjects than those afforded by more traditional (interband) TWV measures.

C. Accuracy of TWV functions

The second major goal of the present study was to evaluate the adequacy of single-exponential curves for describing TWV as a function of cochlear position. This was accomplished by comparing the continuous TWV functions generated by the curve-fitting procedure with estimates of TWV computed directly from ipsilateral wave V latencies. Quantitative comparisons were made for the group mean data; however, informal comparisons of the two measures were also performed for individual subjects. With respect to the mean data, TWV functions derived from the exponential latency functions yielded values that were similar to those for interband velocity estimates, for cochlear sites representing frequencies from 573 Hz to 4.2 kHz. At the most basal site of comparison, namely 7.53 mm from the stapes, TWV functions yielded mean velocity estimates that were lower than those predicted by interband wave V latencies. The significance of this finding is unclear since, as explained above, TWV estimates in this frequency region (approximately 7.1

kHz) may have been contaminated by click-level effects. However, a review of individual subjects' data suggests that this discrepancy may reflect the inability of single-exponential functions to describe response latency precisely in all regions of the cochlea.

Although fits of wave V latency by single-exponential functions were generally excellent for all subjects, an exponential function with equal weights assigned to all points tended to overestimate the slope of the latency-distance function (and underestimate TWV) near the base of the cochlea. The error was small for most subjects, in the sense that fitted function values were only slightly lower than interband velocity estimates at the 7.53-mm cochlear place. However, the error was substantial for a few subjects. It is likely that using a single higher-order function to fit the latency data, or using two separate exponential functions to fit latency data in the cochlear base and apex, respectively, would eliminate this problem and provide a nearly exact fit throughout the length of the cochlea. Alternatively, changing the weighting scheme to give more emphasis to wave V latencies in the cochlear base might allow a single-exponential function to fit high- and mid-frequency latencies better, at the possible expense of degrading the fit at low frequencies.

ACKNOWLEDGMENTS

This work was supported in part by the Lions of Virginia Hearing Foundation, and was completed by GSD in partial fulfillment of requirements for the Ph.D. degree at the University of Virginia. The authors are indebted to Dr. Eric Javel for providing the curve-fitting programs and plotting software that were employed in the data analyses. We are also grateful to Dr. Eric Javel, Dr. Robert Burkard, Dr. Robert Goldstein, and Dr. Chris Van den Honert for providing valuable comments on earlier versions of this manuscript.

Békésy, G. von (**1933**). "Ueber den Knall und die Theorie des Hoerens," Phys. Z. **34**, 577–582.

Békésy, G. von (**1960**). *Experiments in Hearing* (McGraw-Hill, New York).

Békésy, G. von (**1963**). "Hearing theories and complex sounds," J. Acoust. Soc. Am. **35**, 588–601.

Bohne, B. A., and Carr, C. D. (**1979**). "Location of structurally similar areas in chinchilla cochleas of different lengths," J. Acoust. Soc. Am. **66**, 411–414.

Bredberg, G. (**1968**). "Cellular pattern and nerve supply of the organ of Corti," Acta Otolaryngol. Suppl. 236.

Burkard, R. (**1983**). "Far-field electrophysiologic correlates of auditory masking," Ph.D. dissertation, University of Wisconsin.

Dallos, P., and Cheatham, M. A. (**1970**). "Travel time in the cochlea and its determination from cochlear-microphonic data," J. Acoust. Soc. Am. **49**, 1140–1143.

Don, M., and Eggermont, J. J. (**1978**). "Analysis of the click-evoked brainstem potentials in man using high-pass noise masking," J. Acoust. Soc. Am. **63**, 1084–1092.

Don, M., Eggermont, J. J., and Brackmann, D. E. (**1979**). "Reconstruction of the audiogram using brain stem responses and high-pass noise masking," Ann. Otol. Rhinol. Laryngol. Suppl. 57, 1–20.

Eggermont, J. J. (**1976a**). "Analysis of compound action potential response to tone bursts in the human and guinea pig cochlea," J. Acoust. Soc. Am. **60**, 1132–1139.

Eggermont, J. J. (**1976b**). "Electrocochleography," in *Handbook of Sensory Physiology*, edited by W. D. Keidel and W. D. Neff (Springer-Verlag, Berlin), Vol. V/III.

Eggermont, J. J., and Odenthal, D. W. (**1974**). "Frequency selective masking in electrocochleography," Rev. Laryngol. (Bordeaux) **95**, 489–496.

Elberling, C. (**1974**). "Action potentials along the cochlear partition recorded from the ear canal in man," Scand. Audiol. **3**, 13–19.

Greenwood, D. D. (**1961**). "Critical bandwidth and the frequency coordinates of the basilar membrane," J. Acoust. Soc. Am. **33**, 1344–1356.

Gould, H. J., and Sobhy, O. A. (**1992**). "Using the derived auditory brain stem response to estimate traveling wave velocity," Ear Hear. **13**, 96–101.

Hardy, M. (**1938**). "The length of the organ of Corti in man," Am. J. Anat. **62**, 291–311.

Hecox, K., and Deegan, D. (**1983**). "Rise-fall time effects on the brainstem auditory evoked response: Mechanisms," J. Acoust. Soc. Am. **73**, 2109–2116.

Kiang, N. Y. S., Watanabe, T., Thomas, E. C., and Clark, L. F. (**1965**). *Discharge Patterns of Single Fibers in the Cat's Auditory Nerve* (MIT, Cambridge, MA).

Kim, D. O., and Molnar, C. E. (**1979**). "A population study of cochlear nerve fibers: Comparison of spatial distributions of average-rate and phase-locking measures of responses to single tones," J. Neurophysiol. **42**, 16–30.

Liberman, M. C. (**1982**). "The cochlear frequency map for the cat: Labeling auditory-nerve fibers of known characteristic frequency," J. Acoust. Soc. Am. **72**, 1441–1449.

Parker, D. J., and Thornton, A. R. D. (**1978a**). "Frequency specific components of the cochlear nerve and brainstem evoked responses of the human auditory system," Scand. Audiol. **7**, 53–60.

Parker, D. J., and Thornton, A. R. D. (**1978b**). "Cochlear travelling wave velocities calculated from the derived components of the cochlear nerve and brainstem evoked responses of the human auditory system," Scand. Audiol. **7**, 67–70.

Schubert, E. D., and Elpern, B. S. (**1959**). "Psychophysical estimate of the velocity of the traveling wave," J. Acoust. Soc. Am. **31**, 990–994.

Spoendlin, H., and Schrott, A. (**1989**). "Analysis of the human auditory nerve," Hear. Res. **43**, 25–38.

Tasaki, I., Davis, H, and Legouix, J. P. (**1952**). "The space-time pattern of the cochlear microphonics (guinea pig), as recorded by differential electrodes," J. Acoust. Soc. Am. **24**, 502–519.

Teas, D. C., Eldredge, D. H., and Davis, H. (**1962**). "Cochlear responses to acoustic transients: An interpretation of whole nerve action potentials," J. Acoust. Soc. Am. **34**, 1438–1489.

Thornton, A. R. D., and Farrell, G. (**1991**). "Apparent travelling wave velocity changes in cases of endolymphatic hydrops," Scand. Audiol. **20**, 13–18.

Wever, E. G. (**1962**). "Development of traveling-wave theories," J. Acoust. Soc. Am. **34**, 1319–1324.

Zerlin, S. (**1969**). "Travelling-wave velocity in the human cochlea," J. Acoust. Soc. Am. **46**, 1011–1015.